Reproduction of Bifurcation Structure of Belousov–Zhabotinskii Reaction in Flow System by Oscillatory Flow Term Oregonator

Shinji SAKANOUE, Chiaki MURASE,† and Mitsuo ENDO*
Department of Chemistry, Faculty of General Education, Tokyo University of Agriculture and Technology, Saiwaicho, Fuchu, Tokyo 183
† Department of Physics, Faculty of General Education, Tokyo University of Agriculture and Technology, Saiwaicho, Fuchu, Tokyo 183
(Received December 28, 1990)

Simulation has been made on the oscillatory flow term Oregonator model (OFO) proposed in our previous paper for the Belousov–Zhabotinskii reaction (BZ reaction) accompanying constant feed. When the amplitude of the forced oscillation term in OFO is taken extremely small, the computational simulation with this model finely reproduces the oscillatory mode, many types of wave patterns including nonperiodic chaotic behaviors and the bifurcation structure, which appear in the experimental results of the BZ reaction in flow system.

There have been numbers of experimental and theoretical studies[1-5] on the Belousov–Zhabotinskii reaction (BZ reaction) in a continuous-flow stirred tank reactor. Hudson et al.[1] have investigated experimentally BZ reaction in the flow system and found complex phenomena such as several types of periodic multipeak oscillations and chaotic(nonperiodic) behavior. In our previous paper[6,7] for the purpose of reproducing these phenomena by computational simulation, we proposed a model in which a flow term was added to the original Oregonator's equation[8] proposed by Tyson[9], i.e. Oregonator+flow term. Mathematically the model can be expressed by the following differential equations:

$$\mathrm{d}\boldsymbol{X}/\mathrm{d}t = \boldsymbol{O}(\boldsymbol{X}) + R(\boldsymbol{X}^{\mathrm{I}} - \boldsymbol{X}), \tag{1A}$$

where the first term $\boldsymbol{O}(\boldsymbol{X})$ denotes the original Oregonator and the second term $R(\boldsymbol{X}^{\mathrm{I}}-\boldsymbol{X})$ the flow term; or more explicitly,

$$\begin{aligned} \mathrm{d}X/\mathrm{d}t &= (1/\varepsilon)(X + Y - qX^2 - XY) + R(X^{\mathrm{I}} - X), \\ \mathrm{d}Y/\mathrm{d}t &= -Y + fZ - XY + R(Y^{\mathrm{I}} - Y), \\ \mathrm{d}Z/\mathrm{d}t &= (1/p)(X - Z) + R(Z^{\mathrm{I}} - Z), \end{aligned} \tag{1B}$$

where all variables are set dimensionless; and X, Y, and Z are the component of the concentration $\boldsymbol{X}$ corresponding to the concentrations of the three chemical species $HBrO_2$, Br^-, and Ce^{4+}, respectively; and ε, p, and q are the parameters with regard to the rate constants of elementary reactions and f is the paprameter with reference to a stoichiometric coefficient, R corresponds to the flow rate, and t is the time variable. The terms containing R in Eq. 1 are the flow terms to be added to the original Oregonator $\boldsymbol{O}(\boldsymbol{X})$. The X^{I}, Y^{I}, and Z^{I} in them are the components of inflow term $\boldsymbol{X}^{\mathrm{I}}$, and they consist of both the time-independent term $\boldsymbol{X}^0(X^0, Y^0, Z^0)$ and the time-dependent one $\boldsymbol{X}^{\mathrm{I}}(X^{\mathrm{I}}, Y^{\mathrm{I}}, Z^{\mathrm{I}})$:

$$\boldsymbol{X}^{\mathrm{I}} = \boldsymbol{X}^0 + \boldsymbol{X}^{\mathrm{I}}(t), \tag{2A}$$

and the components of $\boldsymbol{X}^{\mathrm{I}}$ are taken as follows

$$\begin{aligned} X^{\mathrm{I}} &= X^0 + Q_x \sin(-\Omega t), \\ Y^{\mathrm{I}} &= Y^0 + Q_y \cos \Omega t, \\ Z^{\mathrm{I}} &= Z^0 + Q_z \sin(-\Omega t), \end{aligned} \tag{2B}$$

where Ω is the angular frequency of the oscillation of the time-dependent term $\boldsymbol{X}^{\mathrm{I}}(t)$, and Q_x, Q_y, and Q_z are the amplitudes of the oscillation of $\boldsymbol{X}^{\mathrm{I}}(t)$. We called the above model the "oscillatory flow term Oregonator" ("OFO"). When $\boldsymbol{X}^{\mathrm{I}}=\boldsymbol{X}^0$, that is the OFO without the time-dependent term $\boldsymbol{X}^{\mathrm{I}}$, we called it the "constant flow term Oregonator" ("CFO"). Here we took the time-independent term $\boldsymbol{X}^0(X^0, Y^0, Z^0)$ to be the steady state of the original Oregonator. Figure 1 shows the three types of global behaviors of the trajectories of CFO projected onto Y–Z plane, which we call the extended state, the intermediate state and the localized state as shown in Fig. 2. In the intermediate state an orbit falls into $\boldsymbol{X}^0$, but a large part of a limit cycle, which we call the semi-global limit cycle, remains around $\boldsymbol{X}^{\mathrm{S}}$. One of the steady state $\boldsymbol{X}^0$ of CFO is common with the steady state of the original oregonator $\boldsymbol{O}(\boldsymbol{X})$ in Eq. 1 and exist for all values of flow rate R. The additional

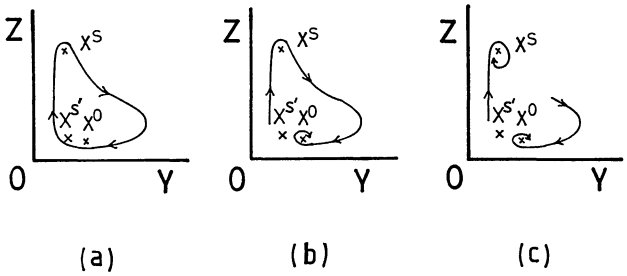

Fig. 1. Schematic representation of three types of behaviors of trajectories of the constant flow term Oregonator (CFO model) in Y–Z plane. $\boldsymbol{X}^0$, $\boldsymbol{X}^{\mathrm{S}}$, $\boldsymbol{X}^{\mathrm{S}'}$; steady states. (a) extended state, (b) intermediate state, and (c) local state.

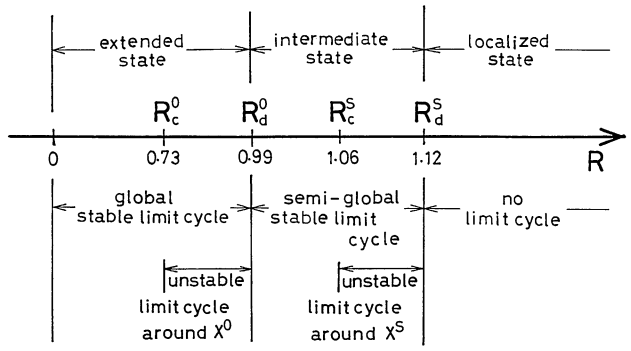

Fig. 2. Relation between three types of global behaviors of CFO and the existence of limit cycles for the ranges of flow rate R.

two steady states X^S and $X^{S'}$ of CFO exist in the flow rate range $0.54<R<5.99$. For the range of the flow rate 0.95—1.10 to be considered later three steady states exist; and consequently, CFO is in a multisteady state. The cross signs in Fig. 1 denote the positions of these three steady states. The CFO can also have a stable and an unstable limit cycle in a certain range of R as shown in Fig. 2.

In the previous paper[6] we showed the behavior of OFO in which the parameters ε, q, f, p, and Ω in Eq. 1 were chosen as follows;

$$\varepsilon = 0.05, \quad q = 0.01, \quad f = 1.8, \quad p = 3 \quad \Omega = 0.75, \quad (3)$$

and the components of the amplitude $\boldsymbol{Q}$ of the forced oscillation in Eq. 2 were set to

$$Q_x = 2, \quad Q_y = 0.5, \quad Q_z = 1. \quad (4)$$

These values of the amplitude $\boldsymbol{Q}$ were chosen about 1/15—1/40 of the amplitude of the stable limit cycle of the original Oregonator. This implies that the forced oscillation very weakly acts in OFO. In order to distinguish the combined parameter set of (3) and (4) from the parameter set in this paper, we call it the "OFO-I". In the previous paper[6] we indicated that the OFO-I could qualitatively exhibit the characteristic features of the experimental results by Hudson et al., but we could not succeed in reproducing the fine details of the oscillatory modes, the wave patterns and the nonperiodic chaotic behaviors which appear in the experiment on the BZ reaction of flow system.

In this study we take the values of the amplitude $\boldsymbol{Q}$ as

$$Q_x = 0.07, \quad Q_y = 0.0175, \quad Q_z = 0.035, \quad (5)$$

which is extremely smaller than the values of (4) of OFO-I. These magnitudes of the amplitude of forced oscillation are about 1/1000—3/1000 of the amplitude of the limit cycle of the original Oregonator, and is about 1/29 of the amplitude of forced oscillation of OFO-I. The other parameters ε, q, p, f, and Ω are set fixed again to the same values of the set (3). We call the OFO with the combined parameter set of (3) and (5) the "OFO-II". The following would show that the simulational results on the OFO-II can exhibit not only the elementary features of the experiment qualitatively, but also a fine agreement with the experimental results on the oscillatory modes, the wave patterns and the nonperiodic chaotic behaviors. Simply speaking the OFO-II can reproduce the detailed bifurcation structure of the flow rate R.

Results

We carry out the computational simulation on the OFO model of the Eq. 1 with the parameter set of the OFO-II, where the magnitudes of the amplitude $\boldsymbol{Q}$ in the time-dependent term X^1 in Eq. 2B are set extremely small values of Eq. 5. The time variation of the OFO-II is determined by the Runge–Kutta Gill's method. The value of the flow rate R is varied by the increase of 0.002 throughout the range of 0.950—1.100, which include both the upper end of the extended state and all the range of the intermediate state of CFO shown in Fig. 2. Figure 3 shows the projections of the typical trajectories of both the OFO-I and the OFO-II onto Y–Z plane, where the three steady states X^0, X^S, and $X^{S'}$ of CFO are marked with the crosses. In the range of R mentioned above, X^0 is a stable focus while X^S changes from an unstable focus to a stable focus, and $X^{S'}$ is a saddle point as shown in Fig. 4. As can be seen from Fig. 3, the orbit of OFO-I turns around X^S while that of OFO-II passes through X^S and turns around X^0. For $0.73<R<0.99$, CFO has an unstable limit cycle around X^0 as shown in Fig. 2. The typical oscillatory wave patterns from the OFO-II are shown in Figs. 5—7 for the series of values of the flow rate R. In these figures the patterns from the experiment by Hudson et al.[1] are also shown for comparison. Here we adopted the abbreviated notations of the mode for oscillatory patterns introduced by Tomita et al.[10] like as; (1) $\Pi(n)$ denotes an n-peaked periodic mode, (2) $\Pi_{l_n,l_m}(n, m)$ a periodic switching between l_n times $\Pi(n)$-like and l_m times $\Pi(m)$-like mode, (3) $\chi(n, m)$ a chaotic switching between $\Pi(n)$-like and $\Pi(m)$-like modes. We introduce the notation $\Pi(S)$ for the periodic oscillation with a small amplitude only.

We have ever summarized the qualitative features of oscillation behaviors of the results of the experiment by Hudson et al.[1] into the following three points; (a) two types of the peaked oscillations, one with a large amplitude and the other with a small amplitude, (b) multi-peaked oscillations with a large amplitude and some small amplitudes, and (c) the mixing of two types of oscillations and the sandwiched structure in the bifurcation structure for the flow rate R. We could express these three features more explicity using the notation of oscillation mode mentioned above; (a) the 2-peaked

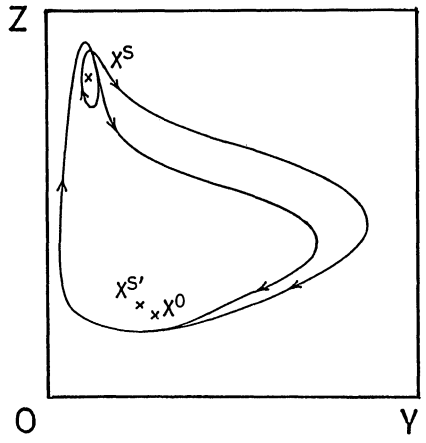

(a) OFO-I Q_x=2.0, Q_y=0.5, Q_z=1.0, R=1.06.

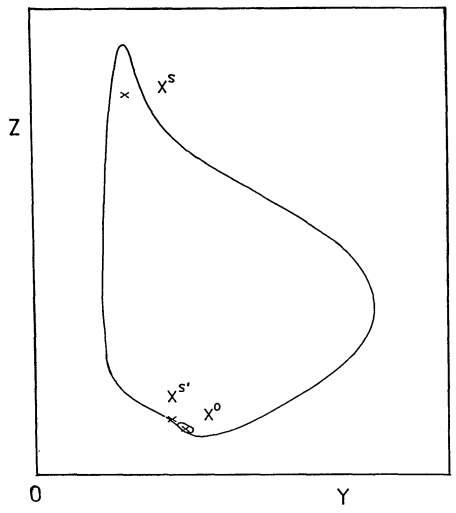

(b) OFO-II Q_x=0.07, Q_y=0.0175, Q_z=0.035, R=1.00.

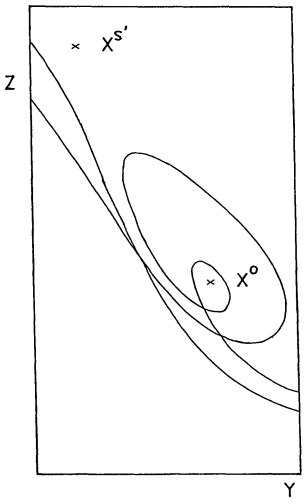

(c) Magnification of orbit around X^0 in (b).

Fig. 3. Typical behaviors of the two types of trajectories in Y–Z plane corresponding to the different two amplitudes in OFO model. X^0, X^S, $X^{S'}$; steady states.

Stationary state	R				
	0	0.54	0.73	0.74	1.06
X^0	UF			SF	
X^S	—	UN		UF	SF
$X^{S'}$	—	S			

Fig. 4. Change of local behaviors of orbits around steady states with varitaion of flow rate R. UF: unstable focus, SF: stable focus, UN: unstable node, S: saddle, —: nonexistence of the stationary state.

oscillation $\Pi(2)$, for example, is composed of one large amplitude oscillation and one small amplitude oscillation, (b) $\Pi(5)$, for example, expresses the 5-peaked oscillation with one of the large amplitude and four of the small amplitude, (c) $\Pi_{1,1}(1,3)$, for example, implies the mixing oscillation of $\Pi(1)$ and $\Pi(3)$, and the sandwiched structure of those two types of modes means that the range of the flow rate R at which $\Pi_{1,1}(1,3)$ appears is sandwiched by the range of $\Pi(1)$ and that of $\Pi(3)$. In the previous paper we have showed that OFO-I can properly exhibit three qualitative features of experimental results. While, as we can see in Figs. 5—7, the OFO-II not only can exhibit the qualitative features (a)—(c) above mentioned, but also can reproduce all kinds of periodic oscillatory modes and wave patterns to be found in the Hudson's experimental results. Only the exception on this correspondence is that the mode $\Pi(4)$ from the experiment could not be found stably in the simulational results, but appear temporarily. For example the mode $\Pi(4)$ sometimes appears near the flow rate R=1.066 and continue to exist for some time, but as time goes on some other modes always mix with $\Pi(4)$ mode. This seems to mean that the mode $\Pi(4)$ cannot exist stably in OFO-II model, and we have judged that $\Pi(4)$ cannot be found in our simulation.

Figure 8 shows the bifurcation structures of oscillatory modes both from the simulation with OFO-II and from the Hudson's experiment. In the figure of the bifurcation structure we put the mark "○" on the value of R at which a periodic oscillation appears, and no mark on the other values of R at which nonperiodic oscillations, i.e. chaotic behaviors, are realized. The simulational results of the bifurcation structure agree very well qualitatively with the experimental one. On this correspondence there are two exceptions that the mode of $\Pi(4)$ can not be found in the simulational results as mentioned above, and the modes $\Pi_{1,1}(1,3)$ and $\Pi(2)$ are situated in reverse order one another on the increase of R value between (a) and (b) in Fig. 8.

From the analysis of the Hudson's experimental data Tomita et al.[10] found that the period T_p of a p-peaked periodic mode obeys a simple rule, namely

$$T_p = T + (p - 1)\tau, \tag{6}$$

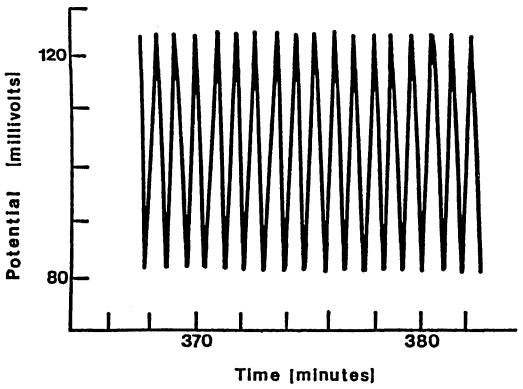

(a-1) Flow rate=2.91 ml min^{-1}

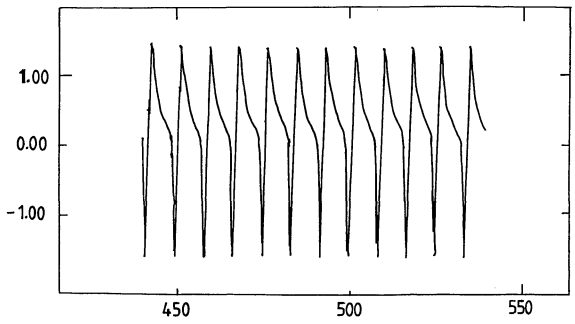

(a-2) $\Pi(1)$, R=0.9520

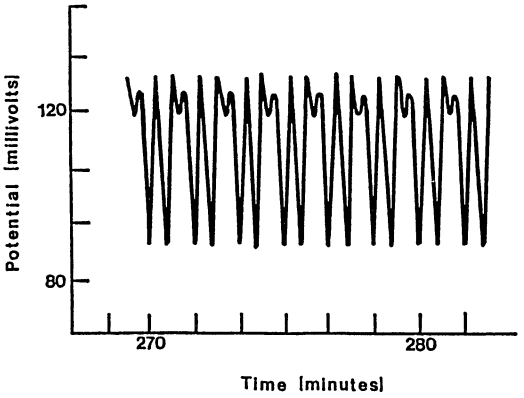

(b-1) Flow rate=3.76 ml min^{-1}

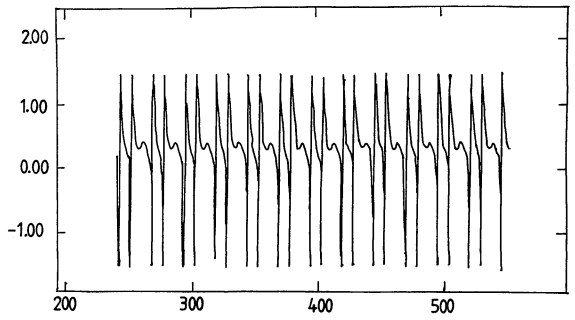

(b-2) $\Pi_{1,1}(1,2)$, R=0.9660

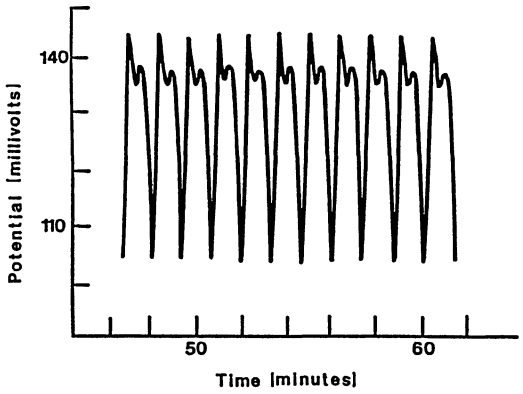

(c-1) Flow rate=4.06 ml min^{-1}

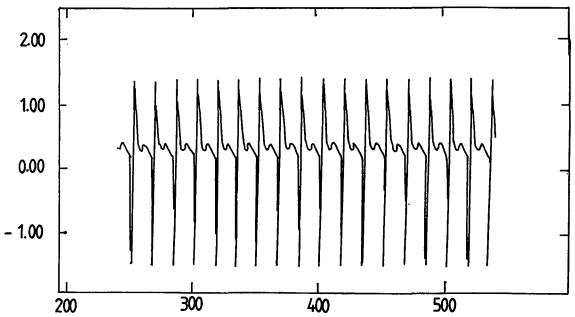

(c-2) $\Pi(2)$, R=1.0240

Fig. 5. Comparison of the wave patterns from OFO-II model (right hand side figures 2) with those from Hudson's experiment of Ref. 1 (left hand side figures 1) for the flow rate. (a-1), (b-1), and (c-1) are recordings from bromide ion electrode; T=25°C; Ce^{3+}catalyst. (a-2), (b-2), and (c-2) are our simulations for Q_x=0.07, Q_y=0.0175, Q_z=0.035.

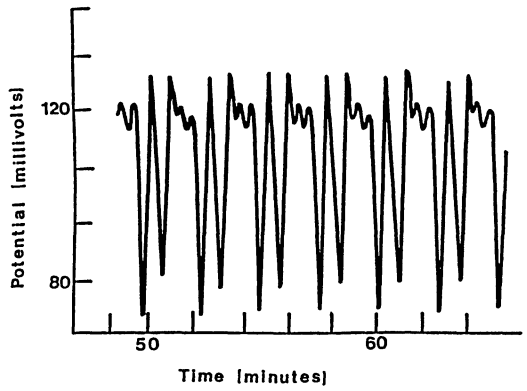

(d-1) Flow rate=3.99 ml min^{-1}

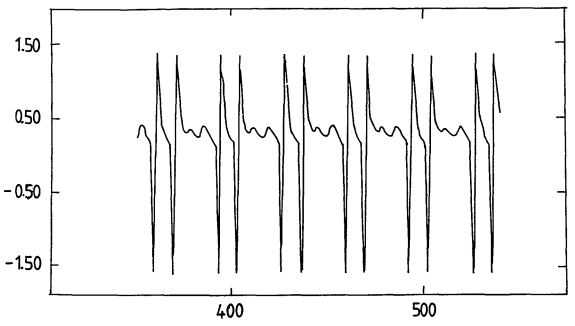

(d-2) $\Pi_{1,1}(1,3)$, R=1.0440

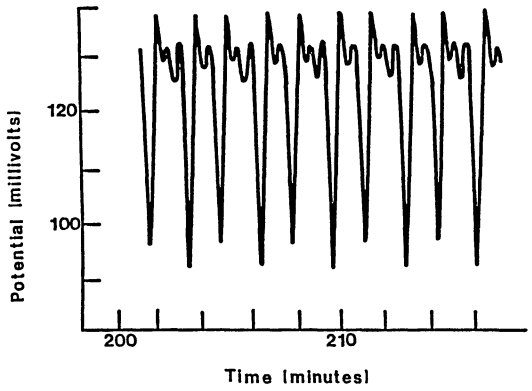

(e-1) Flow rate=4.11 ml min^{-1}

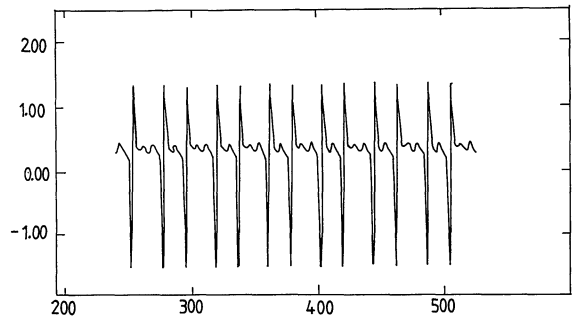

(e-2) $\Pi_{1,1}(2,3)$, R=1.0600

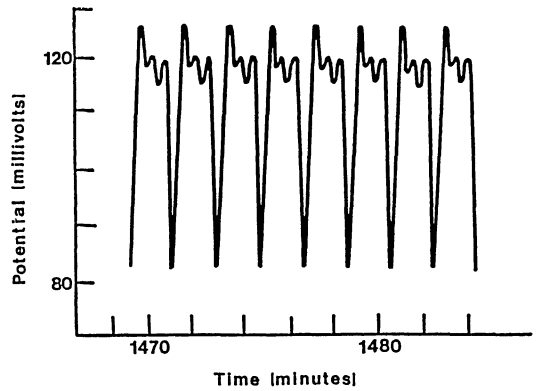

(f-1) Flow rate=4.34 ml min^{-1}

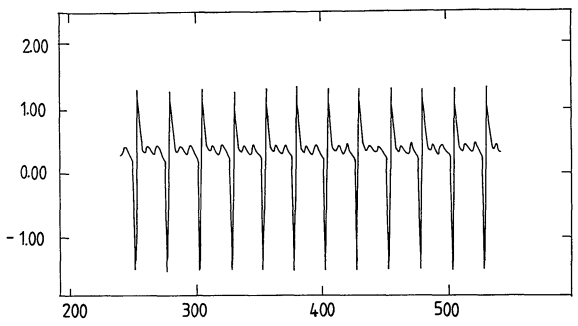

(f-2) $\Pi(3)$, R=1.0800

Fig. 6. Comparison of the wave patterns from OFO-II model (right hand side figures 2) with those from Hudson's experiment of Ref. 1 (left hand side figures 1) for the flow rate. (d-1), (e-1), and (f-1) are recordings from bromide ion electrode; T=25° C; Ce^{3+}catalyst. (d-2), (e-2), and (f-2) are our simulations for Q_x=0.07, Q_y=0.0175, Q_z=0.035.

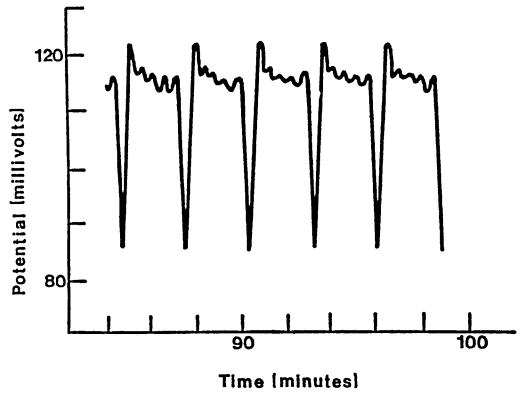

(g-1) Flow rate=4.81 ml min^{-1}

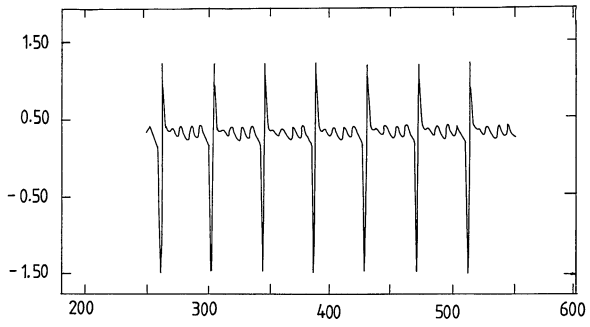

(g-2) $\Pi(5)$, R=1.0902

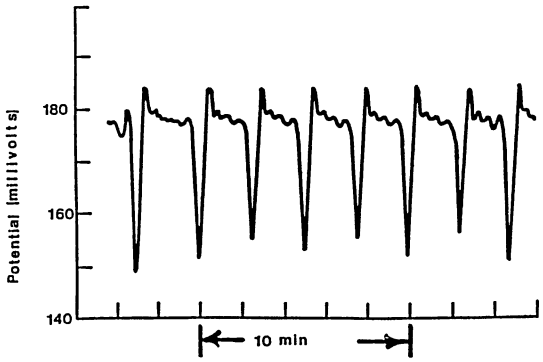

(h-1) Flow rate=4.76 ml min^{-1}

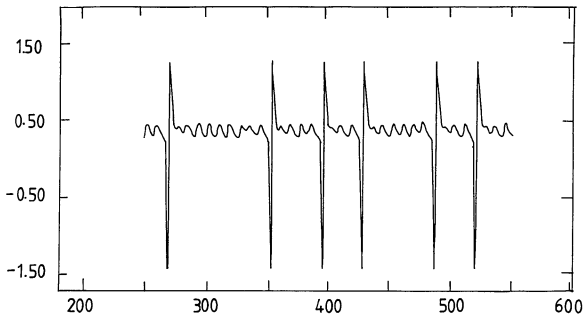

(h-2) χ, R=1.0912

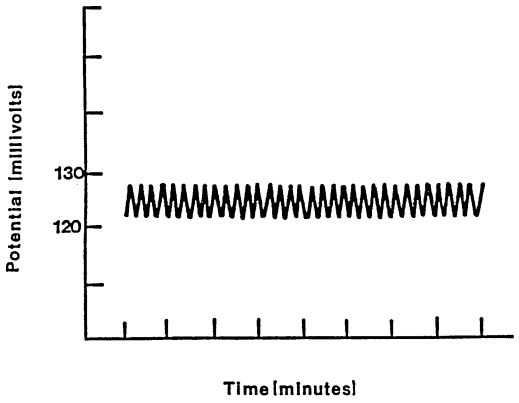

(i-1) Flow rate=5.42 ml min^{-1}

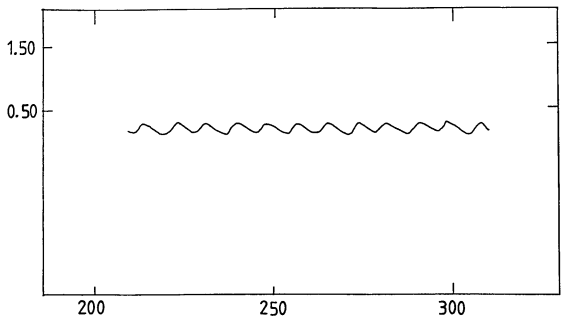

(i-2) $\Pi(S)$, R=1.0980

Fig. 7. Comparison of the wave patterns from OFO-II model (right hand side figures 2) with those from Hudson's experiment of Ref. 1 (left hand side figures 1) for the flow rate. (g-1), (h-1), and (i-1) are recordings from bromide ion electrode; T=25°C; Ce^{3+}catalyst. (g-2), (h-2), and (i-2) are our simulations for Q_x=0.07, Q_y=0.0175, Q_z=0.035.

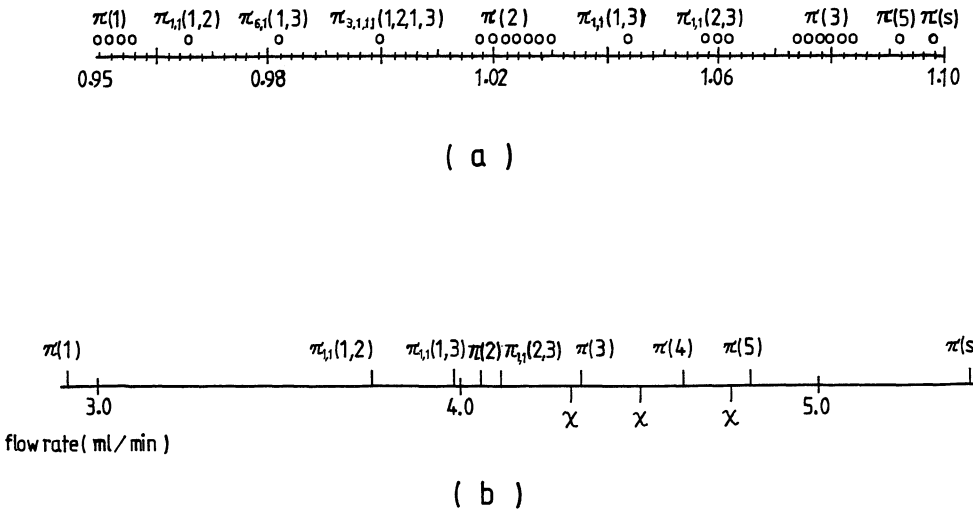

Fig. 8. Bifurcation structure of OFO-II model for flow rate R and its comparison with the Hudson's experimental results of Ref. 1. (a) Bifurcation structure from OFO-II. (b) Bifurcation structure from Hudson's experiment.

Table 1. Periods from Simulations and from Theoretical Formula (6)

Flow rate	Multiplicity	Periods	
R	p in π (P)	T_p(obs)[a]	T_p(theor)[b]
0.952	1	10.41	10.41
1.024	2	16.78	17.81
1.080	3	25.13	25.21
1.090	5	41.93	40.01

a) T_p(obs): period obtained from simulations. b) T_p(theor)= $T+(p-1)\tau$, $T=10.41$, $\tau=7.40$ (6).

where $p=1,2,3,4$, and 5, and both of T and τ are constants. Tomita gave $\tau=0.48$ and $T=0.96\approx 2\tau$. Here, we tried to apply this rule to our simulational data based on OFO-II. When $\tau=7.40$ and $T=10.41$, we confirmed very good agreement between the period predicted from Eq. 6 and the period obtained by the simulation data. The result is indicated in Table 1, where T_p(theor) is the period predicted from Eq. 6 and T(obs) is that of the simulational data. Here the value of $T(=10.41)$ is smaller than $2\tau=2\times 7.40=14.80$ and $\tau(=7.40)$ is also slightly smaller than the value of the period $2\pi/\Omega=8.38$ to be expected from the angular frequency Ω of the oscillation. It is interesting, however, that the every difference is not so large.

Discussion

We studied the behaviors of the oscillatory flow term Oregonator (OFO model) to compare our results with the experimental results of Hudson et al.[1] The simulation of OFO has been made under the values of parameters of OFO-II which is same as OFO-I except the extremely small amplitude of the forced oscillation. It can be concluded that the OFO-II model is very suitable for reproducing the experimental results by Hudson et al.

In the previous paper[6,7] we have shown that the trajectory of CFO changes both globally and locally according to the value of the flow rate R as shown in Fig. 1. And the behavior of CFO is primarily determined by the competitions among some attractors like as steady states and a stable or an unstable limit cycle. We think that these behaviors of CFO still perform a part of the background of the behaviors of OFO because the only difference of OFO from CFO is the existence of the forced oscillation term of which amplitude is set extremely small of order 1/500 compared with the amplitude of the limit cycle of CFO. Therefore, the steady states, X^0, X^S, $X^{S'}$, and the limit cycles in CFO may also be at work as the latent attractors in OFO. In the previous paper we summarized the following conditions for the exhibition of the characteristic features of the Hudson's experimental results by OFO: (1) The CFO, which could be the background of the OFO, should have two steady states X^0 and X^S at least. (2) The stability of steady states X^0 and X^S should become larger with the increase of the flow rate R. (3) The value of R should be taken near the value at which the CFO could realize the intermediate state as shown in Fig. 2. (4) The curved surface formed by the orbits near X^S should be enough flat to be able to form the turning orbit around it.

Here, it is newly confirmed that in order to reproduce more finely the Hudson's experimental results by OFO the following conditions should be added. (5) The amplitude of the oscillation in the time-dependent term

of OFO should be extremely smaller than that of OFO-I. Thus the forced oscillation should be so weak that the trajectory is attracted not to the steady state X^S, but to the steady state X^0 and turns around it. (6) The stability of X^0 should be moderate; or more definitely, the stability of X^0 should be as high as a running orbit can be attracted to X^0 and turns around X^0 while it should be as low as the trajectory finally falls not to the steady state X^0, but comes out to the global stable limit cycle which may surpass X^0 in stability. If an unstable limit cycle exists around X^0, the curved surface formed by the orbit inside this unstable limit cycle should be also flat enough, which is same as the condition (4) around X^S. This circumstance corresponds to the condition that the stability of the focus X^0 should be as low as that mentioned in (6). If the stability of X^0 is comparatively low and at the same time the magnitude of the amplitude Q is larger than a certain threshold, the trajectory passes through near X^0 without turning around it. In this case the oscillatory modes, the wave patterns and the bifurcation structure would differ in fine details from those of Hudson's experimental results.

Here, we must pay attention to the fact that no forced oscillation was set in the Hudson's experimental system[1)] while the OFO has the time-dependent flow term implying a forced oscillation. This is a discrepancy between the Hudson's experimental system and the OFO model. From the microscopic point of view, however, local fluctuation in concentrations of chemical species necessarily comes always into the experimental system. The time-dependent term in OFO could be regarded as a correspondence on this fluctuation. Now, there are two discrepancies between the experimental results and the simulational results based on OFO-II. Namely, one of them is the lack of the mode $\Pi(4)$ in the simulational results and the other is an inversion in the order of the appearance of the mode $\Pi_{1,1}(1,3)$ and $\Pi(2)$ with the increase of R. These discrepancies would be due to the difference between the random fluctuation in the expeprimental system and the trigonometric functional oscillation in the OFO model system. But we think that the discrepancies between two results are not so significant and not so essential because qualitatively the OFO-II shows totally a very good reproduction of the bifurcation structure of the experimental results. If these considerations are appropriate, the simulational results mean that the smaller amplitude of forced oscillation in the OFO model guarantees the better correspondence between the OFO model and the real experimental system. From this point of view it can be said that the OFO-II model may have better correspondence to the experimental system than the OFO-I model.

We would like to thank Dr. A. Kouda for valuable discussion. The authors are much indebted to Dr. J. L. Hudson, Dr. M. Hart, and Dr. D. Marinko for kindly permitting us to quote many figures in their paper of Ref. 1.

References

1) J. L. Hudson, M. Hart, and D. Marinko, *J. Chem. Phys.*, **71**, 1601 (1979).
2) C. Vidal, S. Bachelart, and A. Rossi, *J. Phys.*, **43**, 7 (1982).
3) J. C. Roux, *Physica*, **7D**, 57 (1983).
4) T. Yamaguchi, Y. Yamamoto, and K. Imaeda, *J. Phys. Soc. Jpn.*, **58**, 1550 (1989).
5) T. Yamaguchi, Y. Yamamoto, and K. Imaeda, *J. Phys. Soc. Jpn.*, **59**, 857 (1990).
6) C. Murase, S. Sakanoue, and M. Endo, *Prog. Theor. Phys.*, **77**, 1307 (1987).
7) C. Murase, S. Sakanoue, and M. Endo, *Prog. Theor. Phys.*, **77**, 1319 (1987).
8) R. J. Field and R. M. Noyes, *J. Chem. Phys.*, **60**, 1877 (1974).
9) J. J. Tyson, *J. Chem. Phys.*, **66**, 905 (1977).
10) K. Tomita and I. Tsuda, *Prog. Theor. Phys.*, **64**, 1138 (1980).